FEST3D - A SIMULATION TOOL FOR MULTIPACTOR PREDICTION

C. Vicente[(1)], M. Mattes[(2)], D. Wolk[(3)], H. L. Hartnagel[(4)], J. R. Mosig[(5)], D. Raboso[(6)]

[(1)]Institut für Hochfrequenztechnik, Technical University of Darmstadt
Merckstrasse 25, D-64283 Darmstadt, Germany
Email: quiles@hf.tu-darmstadt.de

[(2)]Laboratoire d'Electromagnétisme et Acoustique (LEMA)
Ecole Polytechnique Fédérale de Lausanne (EPFL), Switzerland
Email: michael.mattes@epfl.ch
www: http://itopwww.epfl.ch/LEMA

[(3)]Tesat-Spacecom GmbH & Co. KG
Gerberstrasse 49, 71522 Backnang, Germany
Email: Dieter.Wolk@tesat.de

[(4)]Institut für Hochfrequenztechnik, Technical University of Darmstadt
Merckstrasse 25, D-64283 Darmstadt, Germany
Email: hartnagel@hf.tu-darmstadt.de

[(5)]Laboratoire d'Electromagnétisme et Acoustique (LEMA)
Ecole Polytechnique Fédérale de Lausanne (EPFL), Switzerland
Email: juan.mosig@epfl.ch
www: http://itopwww.epfl.ch/LEMA

[(6)]European Space Agency (ESA/ESTEC)
2200-AG, Noordwijk, Holland
Email: David.Raboso@esa.int

Abstract

In this paper, a software tool for the calculation of the multipactor threshold in passive components based on rectangular geometry is presented. This software is useful for investigating complex devices from their multipactor properties point of view without taking resort to analytical approaches like the parallel-plate approximation. Moreover, the software tool fully integrates the electromagnetic field computation and the multipactor module allowing the user to perform an electromagnetic characterisation (S-parameters or electromagnetic field) or a multipactor analysis.

The experimental results also obtained in the framework of this investigation fully validate the software developed showing that the standard multipactor curves (ECSS [1]) used by the satellite industry underestimate, in many cases, the breakdown threshold.

INTRODUCTION

As time goes by, the requirements in terms of microwave breakdown (basically, multipactor and corona discharge) of satellite components is becoming more and more restrictive. As a consequence, the design of devices free of microwave breakdown becomes, in many occassions, an extremely challenging task. Therefore, it is desired to have at one's disposal a software tool capable to analyse not only the electromagnetic response of microwave components but also to determine the breakdown power of such structures with a reasonable accuracy.

In this framework, the European Space Agency has started the set up of several activities intended to develop such a software tool. The first of them: "Multipactor and Corona Discharge: Simulation and Design in Microwave Components" (Contract No. 16827/02/NL/EC) is devoted to the investigation of multipactor and corona effects in rectangular waveguide components. This paper describes the achievements related to the multipactor effect research.

The organisation of the paper is as follows: We first briefly describe the software tool to compute the electromagnetic field distribution inside waveguide filters. Then, the approach chosen to predict the multipactor breakdown is outlined. The model presented is tested by means of simulations in particular samples for which the multipactor onset has been obtained experimentally.

ELECTROMAGNETIC FIELD

As mentioned, for an accurate multipactor analysis, it is indispensable to know the electromagnetic field distribution inside the microwave device, e. g. a filter. For this, the software tool FEST 3D (Full-wave Electromagnetic Simulation Tool) recently developed by ESA/ESTEC [2] is used. This software uses a full-wave approach, which assures a high accuracy and efficiency, also for complex geometries like microwave filters, and is based on the integral equation technique [3, 4] and microwave network theory. An analysis example is shown in Fig. 1. It compares measurements and simulation of return and insertion loss of a triple-mode filter, demonstrating a good agreement between theory and measurements. Moreover, the field computation is also possible as shown in Fig. 1 where the surface current together with the geometry of such a filter are displayed. High current values are represented by dark, low values by light grey tones.

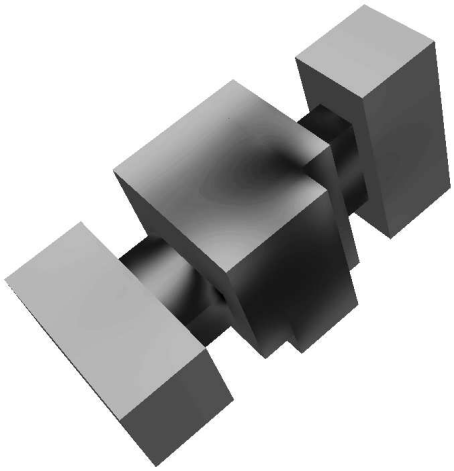

(a) Geometry and Surface current.

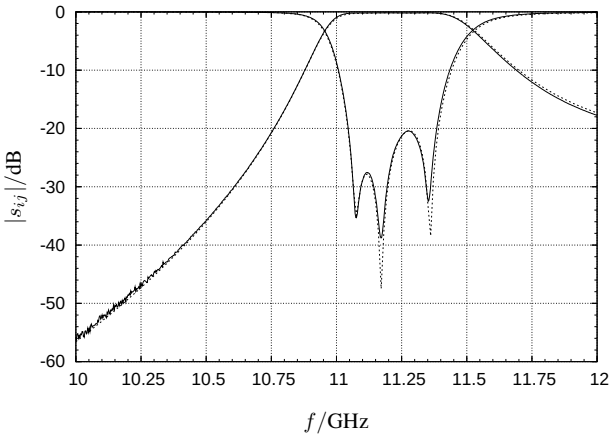

(b) Reflection and transmission coefficients.

Figure 1: Geometry and frequency response of a triple-mode filter. Fig. (a) shows the geometry together with the surface current at 11.2 GHz. Fig. (b) displays the reflection and transmission coefficients. Measurements are drawn in solid lines, simulation results in dashed lines.

Fig. 2 presents the electromagnetic response of one of the samples used for the verification of the multipactor model. It is a transformer gap filter in X-band for which the inner gap element is prone to suffer multipactor due to the high electric field density (see Fig. 2(b)) and to its small height.

MULTIPACTOR

Once the field configuration is known for any point of a particular device, the multipactor simulation can start. A multipactor model/code basically consists of two main parts:

1. Primary electrons generation and electron tracker.
2. Secondary electrons model.

Primary Electrons Generation and Electron Tracker

The primary electrons are located in a particular element of the whole waveguide structure where multipactor needs to be investigated. The initial angle and energy distributions of these primary electrons have been taken randomly in both cases (for the angle values always toward the inner part of the device and energies between 0 and 10 eV), although the properties of the primary electrons hardly affect the breakdown result since the secondary electrons finally describe the electron cloud.
Electrons motion is governed by the 3D Lorentz force equation. In this work, the electron trajectories are found by solving such an equation using a velocity Verlet algorithm which assures sufficient accuracy and good efficiency provided

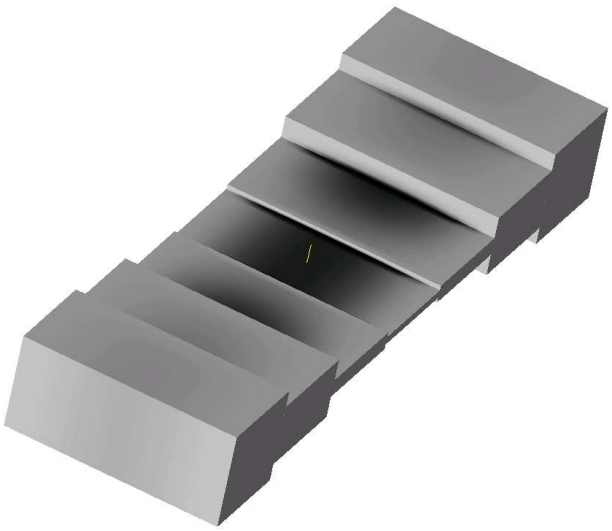

(a) Geometry and Electric field.

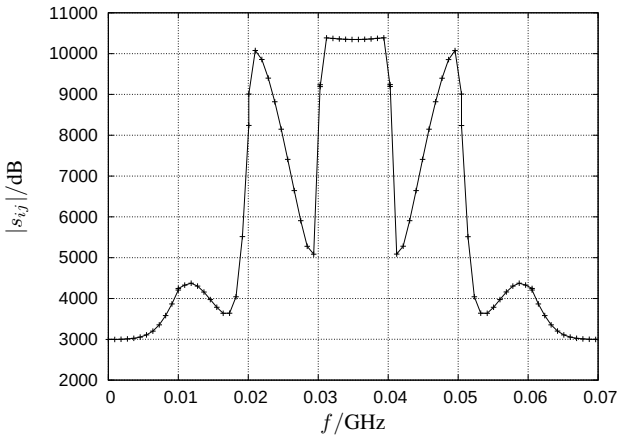

(b) Vertical electric field along centre axis.

Figure 2: Structure used for testing the theoretical approach to predict multipactor. Figure (a) represents the geometry and the electric field distribution and (b) the vertical electric field along the centre axis of the structure. The crosses represent the field values actually computed with FEST 3D. Their straight line interpolation is represented by the solid line. Frequency: 9.5 GHz. Input power: 1 W rms.

enough time steps are chosen. In this case, 100 time steps per RF semiperiod were enough for convergence in the electron trajectory.

Secondary Electrons Model

The electromagnetic field can eventually drive an electron to the waveguide walls. When this happens, this electron can be absorbed, reflected or can extract secondary electrons from the surface. This is basically material dependent and is quantitatively considered by means of the secondary electron emission coefficient (SEEC). The typical curve aspect of this coefficient as a function of the impacting electron energy is shown in Fig. 3 for the low energy range. One of the most commonly used models for the SEEC was formulated by Vaughan [5]. The Vaughan's formula is:

$$\begin{aligned} \delta(E,\theta) &= \delta_{max}(\theta)\cdot(v\,e^{1-v})^k \quad for \quad v \le 3.6, \\ \delta(E,\theta) &= \delta_{max}(\theta)\cdot 1.125/v^{0.35} \quad for \quad v > 3.6, \end{aligned} \tag{1}$$

where

$$v = \frac{E - E_0}{E_{max}(\theta) - E_0},$$

$$k = 0.56 \quad \text{for} \quad v < 1,$$

$$k = 0.25 \quad \text{for} \quad 1 < v \le 3.6,$$

$$\delta_{max}(\theta) = \delta_{max}\cdot(1 + k_E\,\theta^2/2\pi),$$

$$E_{max}(\theta) = E_{max}\cdot(1 + k_\theta\,\theta^2/2\pi),$$

$\delta(E,\theta)$ being the SEEC value for an impacting electron energy E and incident angle θ with respect to the surface normal, $E_0 = 12.5\ eV$, k_E and k_θ parameters dependent on the roughness of the surface (normally taken equal to 1), E_{max} the impact energy at which the SEEC is maximum and δ_{max} the maximum SEEC at this energy.
As seen in (1), the Vaughan curve mainly depends on two parameters: δ_{max} and E_{max}. This leads to two basic problems:

1. At very low energies (below E_0), $\delta(E, \theta)$ is not defined,
2. the first crossover energy at which the SEEC equals to 1 (E_1) is not fitted in the curve.

Low energy impacting electrons are mainly reflected on the surface. This curve does not take into account such a reflection and can not associate a SEEC value for energies lower than E_0. Besides this, and even more important, E_1 is a parameter which considerably affects the multipactor breakdown as already pointed out, among others, by Galán et. al [6] and confirmed by simulations performed by the present authors. In order to overcome such problems, a modified version of the Vaughan's formula has been employed. It is based on adding one more fitting parameter in order to force the SEEC curve to have the first crossover at E_1. To do this, the arbitrarily defined parameter E_0 has been varied until the SEEC curve indeed passes by E_1. Additionally, since at very low energies almost all the electrons are reflected, it has been assumed that the SEEC below E_0 is equal to 1. Thus, for instance, using the ECSS standard values for the SEEC parameters of silver plated ($E_{max} = 165\ eV$, $\delta max = 2.22$, $E_1 = 30\ eV$) and alodine ($E_{max} = 180\ eV$, $\delta max = 1.83$, $E_1 = 41\ eV$) surfaces , curves like those shown in Fig. 3 are obtained. At each electron impact the average number of electrons

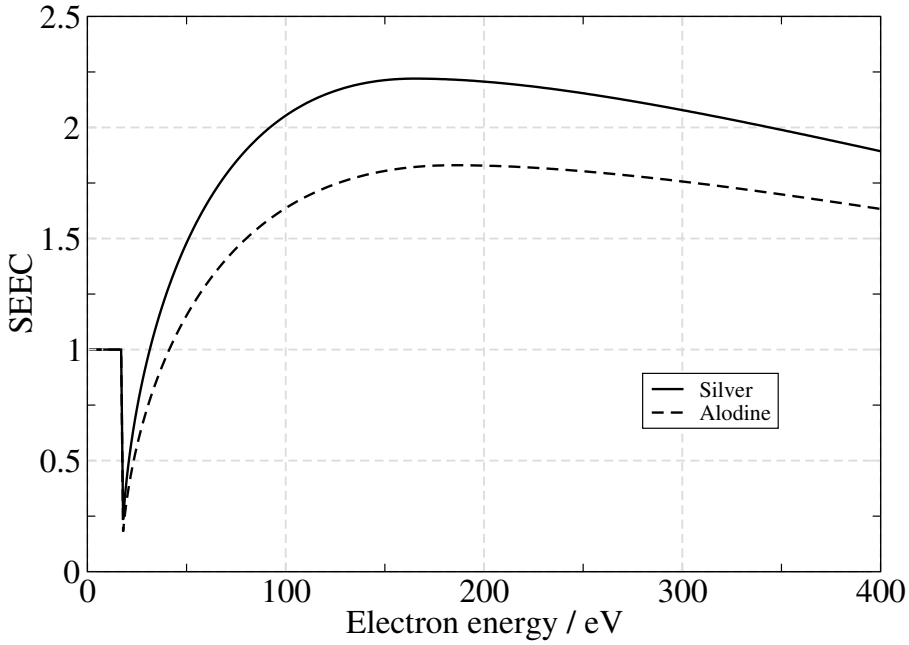

Figure 3: Modified secondary emission curves for silver and alodine. In both cases, the E_0 value which fits E_1 is 17 eV.

generated is given by the SEEC value for the energy and angle of the colliding electron. A well-known approach to model multipactor is to use effective electrons in such a way that the real number of electrons to be tracked remains constant throughout the calculation but each electron represents a larger (or smaller) number of electrons depending on the accumulated SEEC values [7] at each impact. Despite the fact that this approach is extremely useful in many cases and provides reliable results in many geometries [8], it can not be universally employed. Its main drawback comes from the fact that if the length of the device geometry where multipactor is investigated is of the order of the gap height, many electrons can escape from the gap [9]. This makes the effective electron approach unstable since with increasing time, less and less electrons remain in the region of interest and finally, there does not exist sufficient electrons in order to have enough statistics. One can argue that this can be solved just by using more electrons in the simulation. However, this does not improve the whole picture since the multipactor breakdown criterion is normally based on the increase of the electron population with respect to its initial value and hence, to reach the multipactor breakdown condition would again mean that few electrons (compared to the number of primaries) are representing the whole electron sample.

In order to solve this difficulty, one can generate real secondaries each time a collision takes place or absorb the impacting electron. In this work, this procedure has been used in order to be capable to simulate arbitrary structures. In particular, for an electron colliding with a particular energy and angle, a random number of electrons is generated following a Poisson distribution whose average corresponds to the SEEC value. The generated secondaries are emitted following a cosine law distribution for the angle and a Maxwell distribution for their outgoing energy [7].

The remaining issue for having a complete multipactor model is to provide a criterion for deciding whether for an input power a multipactor discharge develops or not. Of course, it is not possible to simulate the real number of electrons and

to stop the simulation when a measurable electron density has been created. Therefore, a multipactor criterion must be defined. The best way to do it in a full numerical approach like ours is to perform numerical experiments to check when the results converge even assuming more restrictive conditions. This has been the procedure followed and it has been taken as multipactor condition that the electron population is doubled with respect to the number of primary electrons. Analogously, one has to provide also a non multipactor criterion. In this case, it has been assumed that multipactor does not occur if the population reduces to the fifth of the number of primary electrons. The non-breakdown condition is more restrictive than the multipactor one because in a whole element a low field region can exist which dramatically reduces the population in this zone whereas multipacting is indeed occurring somewhere else.
All the requirements necessary by a multipactor model have been described. Preliminary tests have been performed by means of four *alodine* transformer X-band samples (see Fig. 2) with different heights for the critical gap. Multipactor has been detected using several methods simultaneously in order to assure that the discharge has taken place. In particular, third harmonic detection and input power nulling have been employed. All tests were done at a frequency of 9.5 GHz. As far as the simulation is concerned, different number of primary electrons were used. It was found that for around 500 electrons the result already converged although this eventually depends on the geometry of the particular device and its field distribution. Fig. 4 shows the results obtained for the multipactor threshold for these four transformers. The Woode and Petit [10] results are based on assuming a parallel plate configuration and are the standard used by the European space community [1]. The multipactor thresholds obtained in this work (FEST 3D) always result in a higher breakdown threshold than the Woode and Petit [10] ones and are very close to the measured data also obtained within the framework of this work. This fully shows the validity of the model presented in this paper. Discrepancies between the results from Woode and Petit and the measured data are probably due to the fact that the real field distribution inside the structure is not considered.

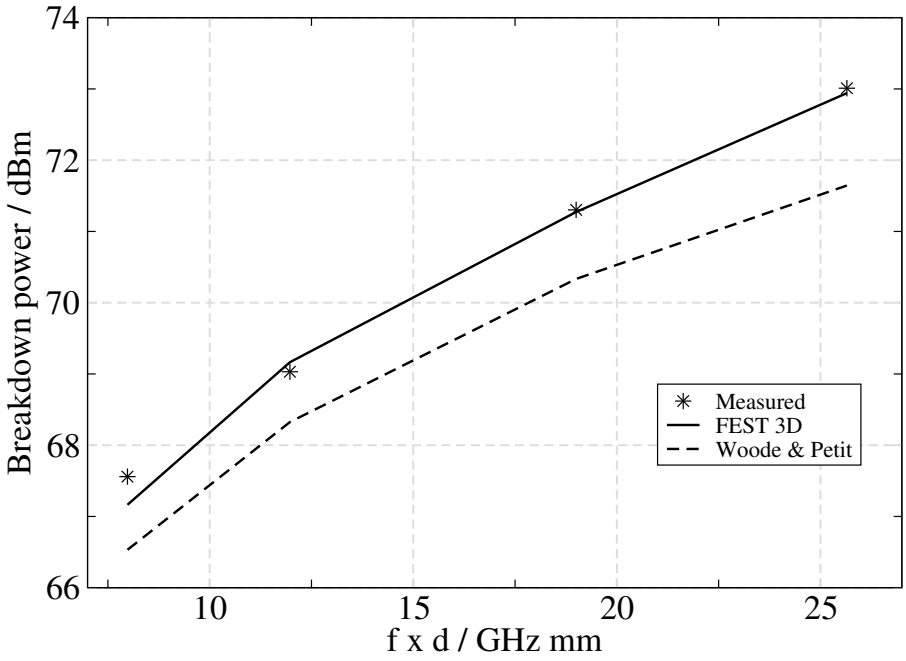

Figure 4: Multipactor threshold for different frequency gap products in alodine. The results obtained in this work (FEST 3D) are in all cases much closer to the measured data than the standard values used by the European SatCom community (Woode & Petit).

The Graphic User Interface (GUI) of FEST 3D is shown in Fig. 5 for the case in which a multipactor simulation is carried out. The user can choose between several standard materials (with the secondary properties defined in the ECSS) or can define new parameters for the SEY. Additionally, the input power at which the power sweep starts can be also selected. This is very helpful when designing particular microwave components since it allows the user to start with the input power given in the multipactor requirements of the device. As a consequence, it can be known relatively fast if the component accomplishes the specifications. The total number of initial electrons to be used in the simulation can be also chosen. Normally, 500 electrons already provide an accurate result. Even for a lower number of electrons, a result close to the final solution can be achieved. In any case, the user can proceed by increasing the number of electrons in different

simulations until the convergence is reached. Finally, the precision of the final result can be also established. Moreover, two different models can be chosen: reduced and full. The reduced model does not consider the magnetic field whereas the full model takes it into account when computing the electron trajectories.

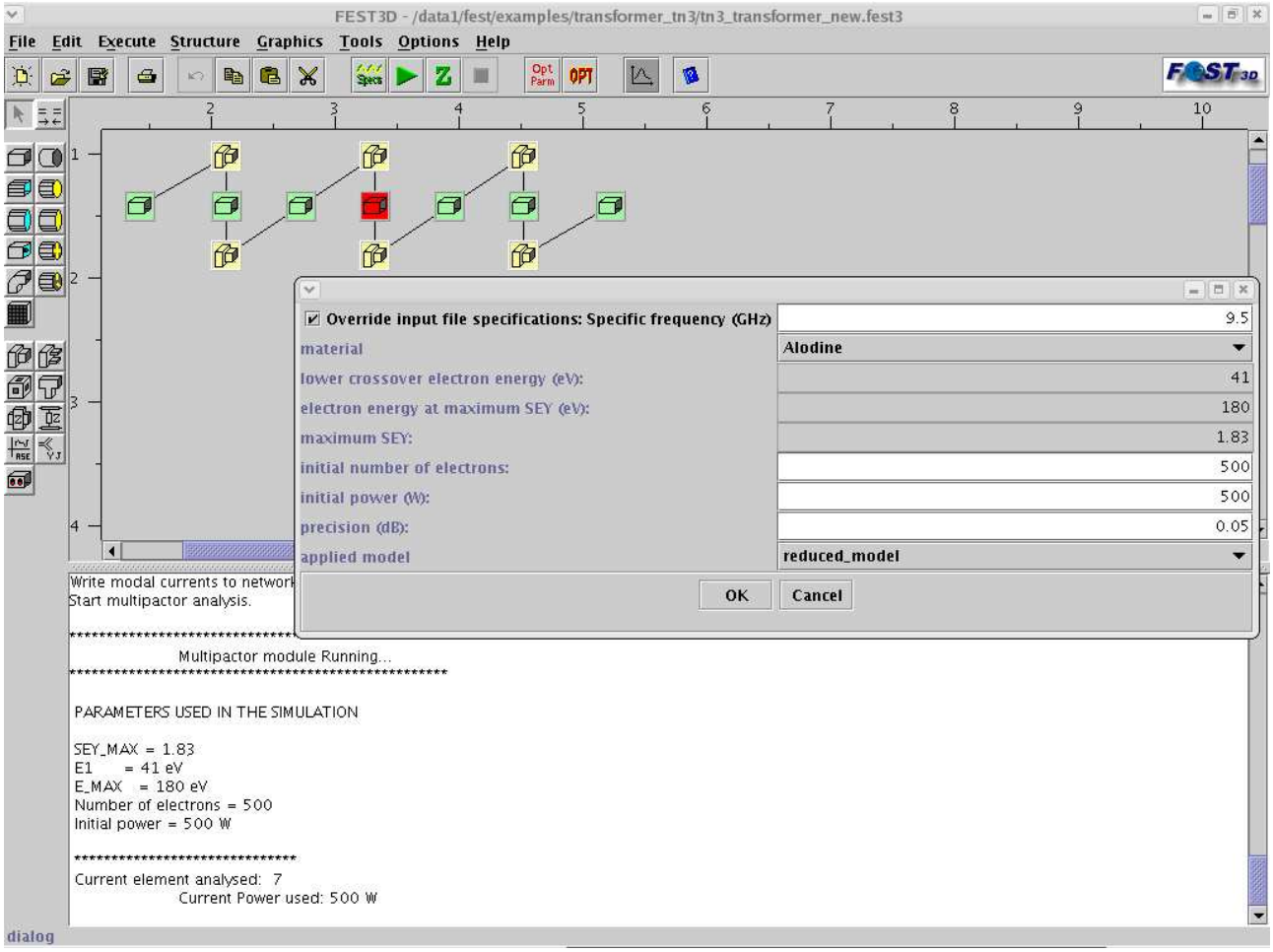

Figure 5: The typical aspect of FEST 3D during a Multipactor simulation.

CONCLUSIONS

A software tool has been presented for the determination of the multipactor breakdown in microwave components based on rectangular waveguide technology. Due to the efficient approach for the computation of the electromagnetic field distribution, this software guarantees the determination of the multipactor threshold in complex components in a reasonable computational time. Additionally, the Vaughan model has been extended in order to fit the first crossover energy as well. Experimental results agree with the simulations performed indicating that the ESTEC curves are very conservative at high $f \cdot d$ products.

ACKNOWLEDGMENTS

This investigation has been financed by the European Space Agency under the project "Multipactor and Corona Discharge: Prediction, simulation and design in microwave components", Contract No. 18827/02/NL/EC. The authors would like to thank Tesat-Spacecom GmbH & Co. KG for providing the experimental data used in this work.

References

[1] "Multipacting design and test", *ESTEC Document ECSS-20-01*, April 2000.

[2] M. Mattes and J. R. Mosig, "Integrated CAD tool for waveguide components, Final Report." Contract ESA/ESTEC No. 12465/97/NL/NB, Dec. 2001.

[3] G. Gerini, M. Guglielmi, and G. Lastoria, "Efficient Integral Equation Formulations for Admittance or Impedance Representation of Planar Waveguide Junctions", *IEEE MTT-S International Microwave Symposium Digest*, vol. 3, pp. 1747–1750, 1998.

[4] M. Mattes, *Contribution to the Electromagnetic Modelling and Simulation of Waveguide Networks Using Integral Equations and Adaptive Sampling*. PhD thesis, Ecole Polytechnique Fédérale de Lausanne, CH-1015 Lausanne, Switzerland, 2003. Thesis No. 2693.

[5] J. Vaughan, "A new formula for Secondary Emission Yield", *IEEE Trans. Electron Devices*, vol. 36, p. 1963, September 1989.

[6] L. Galán, M. A. Jiménez, F. Rueda, and A. Woode, "Development of a Computer Model of the Multipactor Effect", *Final Report ESA/ESTEC Contract 6577*, February 1992.

[7] E. Somersalo, P. Yla-Oijala, and D. Proch, "Electron Mutipacting in RF structures", *TESLA - Collaboration*, July 1994.

[8] E. Somersalo, P. Yla-Oijala, and D. Proch, "Analysis of multipacting in coaxial lines", *IEEE*, pp. 1500–1502, 1996.

[9] A. J. Marrison, "Final Report on the Study of Multipaction in Multi-Carrier Systems", *Report No. AEA/TYKB/31868/RP/2*, July 1994.

[10] A. Woode and J. Petit, "Diagnostic investigations into the multipactor effect, susceptibility zone measurements and parameters affecting a discharge", *ESA- Working paper No.1556*, November 1989.